VII. Applied Mechanics

ENGINEERING MECHANICS DIVISION

A. An Experimental Comparison of Three Typical Mars Entry-Body Shapes on the Basis of Total Equilibrium Shock-Layer Radiation, *H. J. Stumpf*

The AVCO Advanced Research and Development Division, Wilmington, Massachusetts has completed an experimental program for measuring and comparing the total (over the whole body) equilibrium shock-layer radiative heat transfer for three entry-body shapes in a simulated Mars atmosphere. The work was performed under JPL Contract 951331. A description of the test program, entry-body shapes, and experimental facilities is given in SPS 37-40, Vol. IV, pp. 28–31.

The approximate comparison of the equilibrium shock layer radiation was made for the three potential Mars entry body shapes at 0-, 45-, and 90-deg angles of attack by conducting radiation measurements in a shock tube and shock shape measurements in a shock tunnel. Using these data, radiation results were extrapolated to a trajectory condition for the full-size vehicles using a simplified analytical model described in Ref. 1. The extrapolation method was tested by comparing zero-angle-of-attack extrapolated results of the shock tube to the radiation measurements obtained in the ballistic range experiments (which simulated the true entry conditions except for size) and to theoretical predictions. The agreement was found to be satisfactory for the 60-deg blunt cone and *Apollo* shapes; but due to a lack of range data and because the simplified theory may not be valid for the tension shell, the results of the comparison made for that shape are questionable.

The results of the relative, full scale, total radiative heat loads W to the vehicle surface during Mars entry are summarized in Table 1.

Local radiation distribution measurements were performed in the shock tube for a 60-deg blunt cone, using a model instrumented with fiber optics. The results of this test confirmed previous calculations which indicated that the radiation at locations on the body other than at the stagnation point may be higher than at the stagnation point.

Table 1. Relative, full scale, total radiative heat loads to vehicle surface

Angle of attack, deg	$\frac{W_{Apollo}}{W_{cone}}$	$\frac{W_{tension\ shell}}{W_{cone}}$
0	2.9	16.0
45	1.7	1.8
90	3.0	0.7

A more stringent test of the usefulnes of the extrapolation method can be made when the results of theoretical calculations are available (SPS 37-40, Vol. IV, pp. 31–32).

B. Analysis of the Crushing of a Dovetail Phenolic Honeycomb Spherical Impact Limiter, *A. C. Knoell*

1. Background

In the development of unmanned space vehicles considerable emphasis has been placed on the development of energy-dissipating materials and devices capable of protecting scientific payloads during lunar or planetary landings. Conditions of omnidirectional impact have generally required that the payload configuration be spherical. This requirement implies that the energy-dissipating medium possesses spherical curvature capability, thereby giving rise to an impact limiter configuration consisting of a spherical payload encased in an energy-dissipating shell.

A new type of nonhexagonal cell phenolic honeycomb possessing good spherical curvature capability and energy-dissipating characteristics is currently under development (Ref. 2). This honeycomb, known as Dovetail, is shown schematically in Fig. 1. It has a constant cell foil thickness and consists of phenolic resin built up on a glass cloth core. The Dovetail is classified according to cell size (honeycomb "land" dimension L_D), configuration (wing angle ϕ), and bulk density (cell foil thickness t).

2. Object and Scope

The purpose of this analysis is to develop a theoretical method for predicting the static and dynamic response characteristics of a Dovetail phenolic honeycomb spherical impact limiter during vertical crushing against a flat unyielding surface. The static response includes the development of the crushing force as a function of the Dovetail material properties and limiter geometry, and the expression of this force in terms of the crushing depth. The dynamic response includes the prediction of the maximum impact velocity and deceleration experienced by a spherical Dovetail limiter during crushing. Included in the analysis are the effects on response of thickness efficiency (a parameter describing the limit of Dovetail crushability before "bottoming out" occurs) and stress waves generated by high velocity impact of the limiter. The so-called cannonball effect, i.e., the penetration of the payload sphere into the Dovetail honeycomb during impact, is considered by determining the deceleration limit at which this phenomenon occurs. Finally, it is intended that the theoretical results obtained from the static response analysis be compared to experimental results as they become available. Comments will also be presented concerning the physical limitations that must be placed on the analytical limiter model.

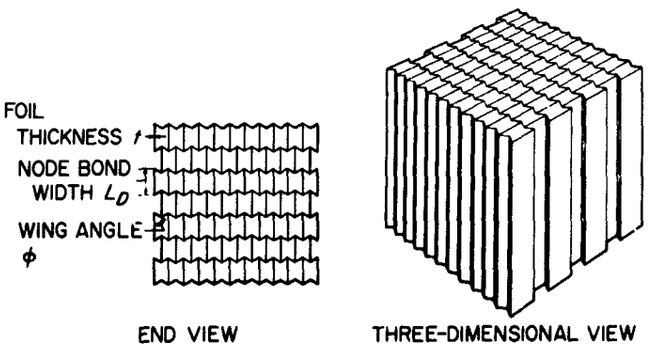

Fig. 1. Sketch of Dovetail phenolic honeycomb specimen

3. Assumptions

In developing the analytical model for a Dovetail impact limiter, it is assumed that the payload is a rigid body and that the cells of the Dovetail honeycomb are geometrically identical and uniformly distributed throughout the impact limiter. This latter assumption implies that spherical geometric symmetry exists, and as a consequence there is no variation in circumferential bulk density of the Dovetail. For small Dovetail cell sizes this assumption is valid since the honeycomb tends to approach a continuous medium. Also, since the Dovetail honeycomb is composed of small cell sizes, it is assumed that continuous functional theory applies. Finally, it is assumed that the Dovetail honeycomb is infinitely rigid in shear and that the only failure mode is crushing of the honeycomb.

4. Analysis Extension

Although not presented here, the analysis has been extended to include both concave and convex surface geometry. The case of rock penetration of the limiter is currently under study. In the future, however, the analysis will be extended to include the effects on response of:

(1) Nonvertical impact

(2) Finite limiter shear stiffness

(3) Nonrigid soil

(4) Nonrigid payload

(5) Nonuniform cell geometry and distribution

5. Analysis Synopsis

The analysis begins with the development of the force at the crushing boundary as a function of angular displacement θ, and is derived from the relation that

$$F_{(\theta)} = \int_{A_{c(\theta)}} \sigma_c \, dA \tag{1}$$

The crushing stress σ_c can be expressed as

$$\sigma_c = \sigma_{c(\rho,a)} \, \xi_{(\phi)} \tag{2}$$

where

$\sigma_{c(\rho,a)}$ = axial crushing stress as a function of Dovetail radial density ρ and cell area a.

$\xi_{(\phi)}$ = reduction parameter to account for decrease in axial crushing stress due to angle of cell loading ϕ.

The terms on the right-hand side of Eq. (2) are derived from experimental data and expressed as algebraic polynomial functions. The Dovetail density, cell area (which combines the effects of cell configuration and size on response), and differential surface area dA are developed as functions of θ and ϕ. Then, by appropriate substitution in Eq. (1), the force at the crushing boundary is developed as a function of θ.

The analysis is continued by deriving the equation of motion which relates the force at the crushing boundary to the deceleration experienced by the impact limiter. To properly account for the stopped mass effect on the deceleration process, the derivation proceeds utilizing principles of fluid mechanics. Specifically, Newton's second law is applied to a system of particles contained within a control volume that is accelerating and has mass crossing its boundaries. The resulting equation, neglecting stress wave effects on response, is

$$F = m_{uc} \ddot{x} \tag{3}$$

where m_{uc} = uncrushed limiter mass, and $\ddot{x}$ = limiter deceleration.

Solving Eq. (3) for the maximum impact velocity that can be attained by the limiter during crushing results in

$$V_c^2 = 2R_L \int_0^{\theta_{max}} \left(\frac{F}{m_{uc}}\right)_\theta \sin\theta \, d\theta \tag{4}$$

where R_L = total limiter radius.

Substituting Eq. (1) in Eq. (4) yields

$$V_c^2 = 2R_L \int_0^{\theta_{max}} \left[\frac{\int_{A_{c(\theta)}} \sigma_c \, dA}{m_{uc}}\right] \sin\theta \, d\theta \tag{5}$$

In Eq. (5) the upper limit of integration θ_{max} is derived from thickness efficiency considerations. The approach taken is to determine that geometric Dovetail cell volume which is just sufficient to house the volume of crushed particles of the centrally-loaded cell. Further loading of the limiter to reduce that geometric cell volume will cause "bottoming out" to occur. The size of the resulting cell volume is therefore a direct measure of thickness efficiency and gives rise to an analytic expression for θ_{max}.

By introducing the concept of a payload fraction, i.e., the ratio of the payload weight to the total limiter weight, in Eq. (5), it is shown that the maximum impact velocity is independent of the limiter mass. It is also shown that the deceleration, as given by the bracketed term of the integrand of Eq. (5), varies as the inverse of the payload radius. In addition to Eq. (5), other design relations pertaining to levels of constant deceleration and limiter size are developed which are also independent of limiter mass. These relations significantly reduce the number of cases to be analyzed for design purposes.

The effect of stress waves on limiter crushing response is developed in a qualitative sense by conservatively determining the number of stress wave reversal cycles occurring in the centrally-loaded Dovetail cell during the total stopping event. It is assumed that if the number of stress wave reversals exceeds ten the solution as given by Eq. (5) is satisfactory since, in effect, it represents the average integrated dynamic response of the limiter.

Finally, an expression is developed for the payload deceleration at which "cannonballing" will occur. Both tensile and compressive forces acting on the payload during deceleration are considered in the development of this expression. In a design sense the results of this relationship are compared to the maximum limiter deceleration to insure that the cannonballing does not occur.

References

1. Reinecke, W. G., and Dyner, H. B., *An Experimental Comparison of Three Typical Mars Entry Body Shapes on the Basis of Total Equilibrium Shock-Layer Radiation,* Final Report JPL Contract 951331, AVSSD-0228-66-RR, AVCO Missiles, Space and Electronics Group, Space Systems Division, Research and Technology Laboratories, Wilmington, Massachusetts, October 10, 1966 (paper submitted for presentation at the *AIAA Thermophysics Specialist Conference*, New Orleans, Louisiana, April 17–20, 1967)

2. *Development of Energy-Dissipating Plastic Honeycomb,* Quarterly Reports 1 through 6, General Electric Co., Space Technology Center, Valley Forge, Pennsylvania, July 1965 through January 1967 (prepared for JPL under Contract 951172).